Elongational Rheology of Polymer Melts and Solutions

JOHN R. COLLIER, OVIDIU ROMANOSCHI, SIMIOAN PETROVAN

Chemical Engineering Department, Louisiana State University, Baton Rouge, Louisiana 70803

Received 19 December 1997; accepted 23 January 1998

ABSTRACT: Elongational rheological properties of polymer melts and solutions may be measured using nonlubricated flow characteristics through a semihyperbolic converging die. The effects of body forces related to developing orientation in the fluid during converging extensional flow are so strong that the shearing contribution become negligible in comparison, eliminating the need for lubrication to achieve an essentially pure elongational flow. The effective elongational viscosities of polypropylene melts and lyocell solutions correlated with shear-flow determinations were used to estimate the enthalpy and entropy changes as function of processing conditions. The flow of lyocell solutions through a converging die had, as a result, not only phase separation and cellulose crystallization, but also microfibers formation and high orientation. © 1998 John Wiley & Sons, Inc. J Appl Polym Sci 69: 2357–2367, 1998

Key words: elongational viscosity; lyocell solution; polypropylene; elongational flow; microfibers; constant strain rate

INTRODUCTION

By contrast to shear rheometry, extensional or elongational rheometry is still in its formative stages. The importance of developing polymer melt and solution elongational rheology measurement techniques is important not only because shear rheological behavior alone is not sufficient to characterize these materials but also because elongational flow is the dominant mode of fluid flow when a rapid change of shape, such as stretching, is involved in an operation. These operations include several important polymer processing operations, including fiber spinning, extrusion through converging profiles, film blowing, and injection molding.[1]

Different approaches have been used for elongational viscosity measurements.[2,3] The main difficulties in studying the elongational rheological properties were reported to be that it is difficult to generate a steady and controlled elongational flow field, and that it is difficult to prevent, compensate, or even measure the shear effects that typically occur simultaneously with the elongational flow. Also, the commercially available elongational rheometers are useful only at elongational rates at least an order of magnitude lower than those encountered in typical industrial processes.[4]

In prior studies accomplished by this research group, a unique technique for characterization of the elongational rheology of polymer melts at processing strain rates has been developed. It was initially demonstrated that an essentially pure elongational flow could be obtained in the core of core–skin coextrusion; this was accomplished experimentally using a core-to-skin viscosity ratio of 30 to 100, and a core-to-skin flow rate ratio of about 10. The high viscosity ratio (core-to-skin) causes the skin layer to act as a lubricating layer.[5–8] Experimental measurements on a pilot scale coextrusion system in a planar slit die using tracer particles and an image analysis system confirmed the predicted behavior and demon-

Correspondence to: J. R. Collier.

Journal of Applied Polymer Science, Vol. 69, 2357–2367 (1998)
 CCC 0021-8995/98/122357-11

strated the ability to achieve a constant elongational strain rate in the core layer.[8]

One of limitation of this rheometer was that the analysis of the core polymer melt requires a choice of appropriate lubricant or skin to be made.[5] In attempting to develop a correction factor for skinless measurements, this study shows that the orienting effect of the polymer melt dominates the flow so strongly that shearing gradients near the wall are insignificant.[9]

MATERIALS AND METHODOLOGY

Polypropylene (PP) and lyocell solutions were used as core materials for the determination of the uniaxial elongational rheological properties. Polyethylene (PE) was used as the skin material for the core–skin PP determinations.

Polypropylene and Polyethylene

The PP used for the experiments was obtained from Phillips (Grade HGX 030). The zero shear viscosity of the PP was 77,382 Pa s at 200°C, and the molecular weight was 300,000, with a polydispersity index between 4 to 6. For the skin-core measurements of elongational viscosities of PP, low-density DOWLEX PE (with the zero shear viscosity of 63 Pa s at 200°C) was used for the outer layer. The melting points obtained using DSC were 164°C for PP and 135°C for PE.

Cellulose and Lignocellulose Lyocell Solutions

Lyocell solutions with concentrations between 2 and 20% (by weight) were obtained by the dissolution of cellulosic and lignocellulosic materials in the *N*-methyl morpholine oxide (NMMO) monohydrate system. Different pretreatments were used to enhance the lignocellulosic materials' ability to form solutions.

A low-molecular-weight recycled cotton (DP $\sim$ 1000) was separated through a novel method from a blend of polyester–cotton after treatment with strong alkali solution.[10] The sugar cane lignocellulosic material rich in cellulose (DP-1100) was extracted from the mechanically separated sugar cane rind using an alkali partial delignification (2 h atmospheric pressure extraction with a 1.75*N* NaOH solution and under continuous mixing) and followed by steam explosion.[11]

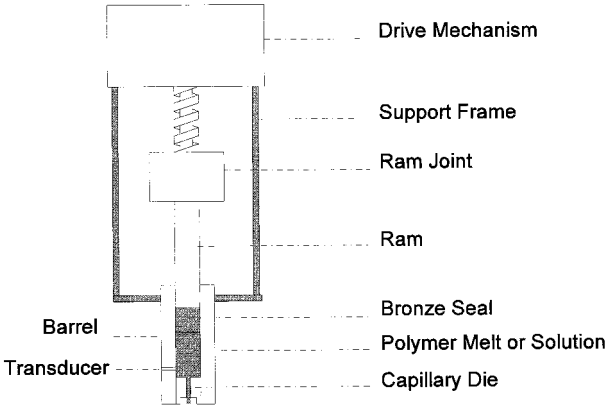

Figure 1 The advanced capillary extrusion rheometer (ACER).

The lyocell solutions were prepared as follows: a 50% NMMO–water solution was mixed with the finely powdered cellulosic or lignocellulosic material and with the antioxidant (*n*-propyl-gallate), in order to control the degradation of both cellulose and NMMO.[12] The monohydrate lyocell system was obtained by distilling water under continuous mixing and vacuum at a moderate temperature range between 80–95°C. The lyocell solutions obtained were optically observed using an Olympus Optical Microscope between crossed polarizers. In addition, a Cambridge StereoScan 260 scanning electron microscope (SEM) was used to observe the fibers obtained from the collected extrudates.

As reported in the literature, liquid crystalline phases appear for both cellulose and lignocellulose systems under certain conditions of concentration and temperature.[13,14] A Seiko 220 differential scanning calorimeter (DSC) was used to measure the enthalpic effect around the transition temperatures. Shear rheological properties of the lyocell solutions were determined with a Haake RS 150 Rheometer using rotational parallel plates. All shear and elongational rheological measurements were performed between 75°C (the melting point for the NMMO monohydrate is 74°C) and 110°C (above this temperature, it is difficult to control the water content).

The determination of the uniaxial elongational rheological properties of polymer melts and concentrated solutions was done using a Rheometric Scientific Advance Capillary Extrusion Rheometer (ACER) by replacing the capillary cylindrical die with semihyperbolic converging axis-symmetric dies (Fig. 1). These electrodischarge-machined (EDM) semihyperbolic convergent conical dies

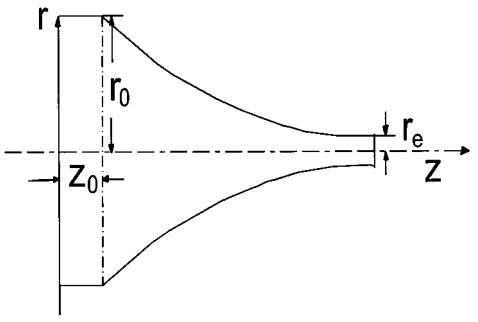

Figure 2 Semihyperbolic convergent die.

were designed to generate a constant elongational strain rate throughout the core; to accomplish this, the flow channel decreases as $R^2z = C_1$, where z is the flow direction, and R is the radius of the flow channel (Fig. 2). Two conical dies are being used having Hencky strains, ϵ_h, of 6 and 7; ϵ_h = ln (area reduction). Elongational strain rates up to 533 s^{-1} have been achieved in this rheometer (the range includes processing rates). The elongational (or shear) strain rates were achieved in steps of ram speeds, with each strain rate corresponding to a fixed ram speed.

When the ACER is used to measure the shear viscosities and for the skinless elongational viscosities, the barrel is filled with the polymer or polymer solution directly into the preheated barrel. For skin–core elongational viscosity measurements, the preheated barrel is filled with a specially prepared billet, with the outer diameter exactly matching the inside diameter of the barrel. The billet is a two-layer concentric cylinder (with the polymer to be analyzed in the core completely encapsulated by the skin). The billets were prepared as described in a previous study.[6]

For the skinless and skin–core PP determinations, a 20-min heat soak was allowed for the samples to reach a thermal steady state prior to experiments' start. This period was reduced to 5 min in the case of lyocell solutions to prevent possible degradations.

Temperature was kept constant for each run, and the pressure drop across the die was recorded. Elongational viscosities were determinated separately on a spreadsheet, after pressure and ram speeds smoothing. For the shear viscosity measurements, direct data were extracted using the ACER software capabilities.

Good control of flow rate and temperature makes possible the use of ACER not only as a measurement device but also as a mini-extruder for fiber spinning from lyocell solutions. Samples of some of the extrudates were collected immediately after the ACER die in a cold water bath. A SEM was used to observe the fibers obtained from the collected extrudates.

THEORETICAL DEVELOPMENT

Analysis of this flow was accomplished using the measured pressure and volumetric flow rate data and mass, momentum, and energy balances. The die shapes were defined realizing that since the interface between the polymer melt or solution and either the die wall for skinless, or if used a lubricating skin, must be a stream tube, that is, a set of streamlines all experiencing the same conditions, including the same value of the stream function, Ψ, and forming a two-dimensional surface. The stream function, in turn, must satisfy the continuity equation; and the potential function, Φ, which can be defined for shear free flows, must be orthogonal to Ψ and satisfy the irrotationality equation. Constant values of the potential function should define surfaces of constant driving force in the systems, that is, constant pressure surfaces. As given below, the stream function and potential function that satisfy these conditions in converging cone geometries and give a constant elongation strain rate are semihyperbolic and mutually orthogonal. A parallel development has been accomplished for the converging slit geometry (the appropriate Ψ and Φ are given in Collier and Perez[15]); but since it results in the same viscosity equations, the slit development is not given in detail, but specific key aspects are mentioned. For cylindrical coordinates, the stream function,

$$\Psi = -\frac{\dot{\epsilon}}{2} r^2 z \tag{1}$$

and the potential function,

$$\Phi = \dot{\epsilon}\left(\frac{r^2}{4} - \frac{z^2}{2}\right) \tag{2}$$

describe the system, with the pressure being directly proportional to $\rho\ \dot{\epsilon}\ \Phi$, where $\dot{\epsilon}$ is the elongational strain rate and ρ is the density. The velocities are

$$\nu_z = -\frac{1}{r}\frac{\partial \Psi}{\partial r} = -\frac{\partial \Phi}{\partial z} = \dot{\epsilon} z \tag{3}$$

$$\nu_r = \frac{1}{r}\frac{\partial \Psi}{\partial z} = -\frac{\partial \Phi}{\partial r} = -\frac{\dot{\epsilon}}{2} r \tag{4}$$

and the nonzero velocity gradients are

$$\frac{\partial \nu_z}{\partial z} = \dot{\epsilon}, \frac{1}{r}\frac{\partial (r\nu_r)}{\partial r} = -\dot{\epsilon}, \frac{\partial \nu_r}{\partial r} = -\frac{\dot{\epsilon}}{2} \tag{5}$$

The basic equations describing the flow are the scalar equations of continuity (that is, mass balance) and a form of energy balance expressed in terms of enthalpy per unit mass, $\hat{H}$; the first-order tensor (that is, the vector), momentum balance; and for potential flow, the irrotationality equation. (In the following, it should be noted that unless otherwise indicated, that the analysis applies to both the skinless flow and to the core material in the skin–core lubricated flow.) Mass, momentum, and energy are conserved separately. The following equations in tensor notation are adapted from Bird et al.,[16] except with the flow in the positive z direction, as in Macosko[2] and Ferguson and Kemblowski.[4] Continuity equation (mass balance),

$$\frac{D\rho}{Dt} = -\rho(\underset{\sim}{\nabla} \cdot \underset{\sim}{\nu}) \tag{6}$$

Momentum balance

$$\rho \frac{D}{Dt} \underset{\sim}{\nu} = -(\underset{\sim}{\nabla} P) + [\underset{\sim}{\nabla} \cdot \underset{\approx}{\tau}] + \rho \underset{\sim}{g} \tag{7}$$

Energy balance

$$\rho \frac{D\hat{H}}{Dt} = -(\underset{\sim}{\nabla} \cdot \underset{\sim}{q}) + (\underset{\approx}{\tau} : \underset{\sim}{\nabla} \underset{\sim}{\nu}) + \frac{DP}{Dt} \tag{8}$$

Irrotationality equation

$$\underset{\sim}{\nabla} \times \underset{\sim}{\nu} = 0 \tag{9}$$

where

$$\frac{D}{Dt} = \frac{\partial}{\partial t} + \underset{\sim}{\nu} \cdot \underset{\sim}{\nabla}$$

and in cylindrical coordinates,

$$\underset{\sim}{\nabla} = \underset{\sim}{\delta}_r \frac{\partial}{\partial r} + \underset{\sim}{\delta}_\theta \frac{1}{r}\frac{\partial}{\partial \theta} + \underset{\sim}{\delta}_z \frac{\partial}{\partial z} \tag{10}$$

where $\underset{\approx}{\tau}$, a second-order tensor, is the stress, and the first-order tensor (that is, the vector) quantities $\underset{\sim}{\nu}$ and q are the velocity and energy flux, respectively. The body force term, g, a first-order tensor, primarily represents the force necessary to orient the material; this term would include a gravitational force if that were significant. The scalar terms P, ρ, and $\hat{H}$ are the pressure, density, and enthalpy per unit mass, respectively.

The geometry of the hyperbolic dies used in this research were chosen to force the elongational strain rate (noted earlier as $\dot{\epsilon}$) to be a constant value determined by the geometry and the volumetric flow rate. The only velocity gradients in this essentially pure elongational flow are in the flow and transverse directions; therefore, the only nonzero components of the deformation rate second-order tensor, $\underset{\approx}{\Delta}$, are the normal components. Since the fluid is assumed to be incompressible, then $\underset{\sim}{\nabla} \cdot \underset{\sim}{\nu} = 0$; therefore, the components of $\underset{\approx}{\Delta}$ are defined in Cartesian coordinate and for i and j being r and z in cylindrical coordinates as

$$\Delta_{ij} = \left(\frac{\partial \nu_i}{\partial x_j} + \frac{\partial \nu_j}{\partial x_i}\right) \tag{11}$$

and

$$\Delta_{\theta\theta} = 2\left(\frac{1}{r}\frac{\nu_\theta}{\partial \theta} + \frac{\nu_r}{r}\right) \tag{12}$$

in cylindrical coordinates. The extra term, ν_r/r, in the $\Delta_{\theta\theta}$ term arises due to the dependence of the unit vector in the r direction upon position. As a result, in Cartesian coordinates, the only nonzero components are the flow and transverse components, Δ_{zz} and Δ_{xx} respectively, $\Delta_{zz} = -\Delta_{xx} = 2\dot{\epsilon}$. The corresponding nonzero components in cylindrical coordinates are Δ_{zz}, Δ_{rr}, and $\Delta_{\theta\theta}$, where Δ_{zz} is the flow direction; $\Delta_{zz} = -2\Delta_{rr} = -2\Delta_{\theta\theta} = 2\dot{\epsilon}$. (Note that $\Delta_{\theta\theta}$ and the corresponding stress tensor component $\tau_{\theta\theta}$ are both nonzero.)

The basic assumptions in this analysis and the related implications are as follows:

1. The stress state in the fluid is uniquely determined by the strain rate state; for example, the fluid could be described by a generalized Newtonian constitutive equation (not a Newtonian fluid), a Herschel-Bulkley material, and so on. Since the geometry dictates that the only nonzero deformation rate components in the essentially shear free flow region are the normal components, and, further, that the deformation rate components are not a function of position, then the only nonzero stress components are the normal components and the stress components are not a function of position. Therefore, $\underset{\sim}{\nabla} \cdot \underset{\approx}{\tau} = 0$.
2. The fluid is incompressible; therefore, $\underset{\sim}{\nabla} \cdot \underset{\sim}{v} = 0$.
3. The system is isothermal; therefore, $\underset{\sim}{\nabla} \cdot q = 0$.
4. The flow is steady; therefore $\frac{\partial}{\partial t} = 0$.
5. The inertial terms are negligible, therefore, $\underset{\sim}{v} \cdot \underset{\sim}{\nabla} \underset{\sim}{v} = 0$, and $\underset{\sim}{\nabla} \left(\frac{\nu_2}{2}\right) = 0$.

Since the convergence of the flow channel was designed to force a constant elongational strain rate, the longitudinal and transverse normal components of the stress tensor, that is, τ_{zz} and τ_{rr}, are also constant, and their values controlled by $\dot{\epsilon}$. If the analysis were for lubricated flow, the shear stress gradients in the core would be assumed to be negligible. It is shown below by the experimental data that the body force $\underset{\sim}{g}$ is dominant and causes the shear stress gradient to also be negligible in skinless flow. Therefore, the stress gradient terms $\underset{\sim}{\nabla} \cdot \underset{\approx}{\tau}$ for both lubricated and skinless flow in the momentum balance equation are negligible, and the inertial terms $\rho \frac{D}{Dt} \underset{\sim}{v}$ are also negligible (the pressure gradients calculated from them alone were 2 to 3 orders of magnitude lower than observed and were independent of fluid character). Using these assumptions, the solution to the momentum balance reveals that the body force $\underset{\sim}{g}$ is equal to $\underset{\sim}{\nabla} P$; that is, in cylindrical coordinates,

$$g_z = \frac{\partial P}{\partial z} \text{ and } g_r = \frac{\partial P}{\partial r} \tag{13}$$

The pressure should be directly proportional to the potential function, Φ. Since the pressure is the driving force, then the proper form, to be dimensionally correct, must have the same form as indicated above; that is, P is directly proportional to $\rho\, \dot{\epsilon}\, \Phi$ and should have the following form:

$$P = A\rho\dot{\epsilon}\Phi + B = P_0 \left[\frac{\left(\frac{r^2}{2} - z^2\right) + \left(L^2 - \frac{r_e^2}{2}\right)}{\left(\frac{r_0^2}{2} - \frac{r_e^2}{2} + L^2\right)} \right] \tag{14}$$

The variables r_o and r_e are the entrance and exit radius values, respectively; L is the centerline length of the die; and P_o is the entrance pressure.

The stress term in the energy balance equation is as follows for cylindrical coordinates:

$$\underset{\approx}{\tau} : \underset{\sim}{\nabla} \underset{\sim}{v} = \frac{3}{2} \tau_{zz} \dot{\epsilon} \tag{15}$$

and for Cartesian coordinates,

$$\underset{\approx}{\tau} : \underset{\sim}{\nabla} \underset{\sim}{v} = 2\tau_{zz} \dot{\epsilon} \tag{16}$$

Using the above basic assumptions, the other 2 possibly nonzero terms in the energy balance are $\rho \frac{D\hat{H}}{Dt}$ and $\frac{DP}{Dt}$, which, with the steady flow assumption, become $\rho\, \underset{\sim}{v} \cdot \underset{\sim}{\nabla} \hat{H}$ and $\underset{\sim}{v} \cdot \underset{\sim}{\nabla} P$. In cylindrical coordinates,

$$\underset{\sim}{v} \cdot \underset{\sim}{\nabla} P = \nu_r \frac{\partial P}{\partial r} + \nu_z \frac{\partial P}{\partial z} \tag{17}$$

The effect of this can be shown by realizing that P is directly proportional to Φ and then integrating from $r = 0$ to r_i (r_i is the value of r at the interface either between the polymer and the die wall in skinless or between the polymer and the skin in lubricated flow and is a function of z, although r is not) and then from $z = 0$ to L. The result is that the first term is negligible since it is proportional to r_e^2 and the second term is proportional to L^2 (the first term is 3 orders of magnitude lower than the second). The same result occurs in Cartesian coordinates. In cylindrical coordinates,

$$\rho \underset{\sim}{v} \cdot \underset{\sim}{\nabla} \hat{H} = \rho \nu_r \frac{\partial \hat{H}}{\partial r} + \rho \nu_z \frac{\partial \hat{H}}{\partial z} \tag{18}$$

By doing a similar double integration, it can be shown that the ν_r value is 2 orders of magnitude lower than ν_z; furthermore, $\frac{\partial \hat{H}}{\partial r}$ should be significantly lower than $\frac{\partial \hat{H}}{\partial z}$ since these terms are related to orientation development in a stretching plug flow and possible heat transfer. Since the flow is occurring inside the temperature-controlled die, the heat transfer in the transverse direction would be negligible, and the fluid is being stretched as a plug in the flow direction; therefore, the gradient in the transverse direction would be significantly smaller than is the longitudinal. The same results occur for these pressure and enthalpy terms in Cartesian coordinates. As a result of these simplification, the energy balance expressed in terms of enthalpy becomes

$$\rho \nu_z \frac{\partial \hat{H}}{\partial z} = + \frac{3}{2} \tau_{zz} \dot{\epsilon} + \nu_z \frac{\partial P}{\partial z} . \tag{19}$$

Since

$$\nu_z = \dot{\epsilon} z \tag{20}$$

and

$$\epsilon_h = \ln\left(\frac{z_e}{z_0}\right) = \ln\left(\frac{r_0^2}{r_e^2}\right) \tag{21}$$

the energy balance can be integrated from the entrance to the exit. Therefore the stress component in cylindrical coordinates is

$$\tau_{zz} = + \frac{2}{3} \frac{\Delta P}{\epsilon_h} + \frac{2}{3} \frac{\rho \Delta \hat{H}}{\epsilon_h} = + \frac{2}{3} \frac{\Delta P}{\epsilon_h} + \frac{2}{3} \frac{\Delta H}{\epsilon_h} \tag{22}$$

where ΔP is defined as entrance minus exit pressure, but ΔH is defined in the normal fashion of exit minus entrance and is the enthalpy change per unit volume, and $\rho \Delta \hat{H} = \Delta H$, where H is the enthalpy per unit volume; in Cartesian coordinates, this term is

$$\tau_{zz} = + \frac{1}{2} \frac{\Delta P}{\epsilon_h} + \frac{1}{2} \frac{\rho \Delta \hat{H}}{\epsilon_h} = + \frac{1}{2} \frac{\Delta P}{\epsilon_h} + \frac{1}{2} \frac{\Delta H}{\epsilon_h} \tag{23}$$

The elongational viscosity term, η_e, in cylindrical coordinates is defined and results in this geometry as follows:

$$\eta_e = \frac{\tau_{zz} - \tau_{rr}}{\dot{\epsilon}} = \frac{3}{2} \frac{\tau_{zz}}{\dot{\epsilon}} \tag{24}$$

In Cartesian coordinates,

$$\eta_e = \frac{\tau_{zz} - \tau_{xx}}{\dot{\epsilon}} = 2 \frac{\tau_{zz}}{\dot{\epsilon}} \tag{25}$$

Therefore, in both Cartesian and cylindrical coordinates, the elongational viscosity is

$$\eta_e = \frac{\Delta P}{\dot{\epsilon} \epsilon_h} + \frac{\rho \Delta \hat{H}}{\dot{\epsilon} \epsilon_h} = \frac{\Delta P}{\dot{\epsilon} \epsilon_h} + \frac{\Delta H}{\dot{\epsilon} \epsilon_h} \tag{26}$$

The enthalpy term would represent either a real or apparent phase change that may be induced by the imposed orientation on the polymer melt or solution.

The definition of the effective elongational viscosity, η_{ef}, and its relation to η_e in both Cartesian and cylindrical coordinates is as follows:

$$\eta_{ef} \equiv + \frac{\Delta P}{\dot{\epsilon} \epsilon_h} \tag{27}$$

$$\eta_e = \eta_{ef} + \frac{\Delta H}{\dot{\epsilon} \epsilon_h} \tag{28}$$

This definition of η_{ef} assumes that any enthalpy change is included in this and, except for the term ϵ_h, is similar to the instantaneous elongational viscosity for the spin–line rheometer,[4] in which the stress term is equal to ΔP. In these expressions, ΔP is the pressure gradient, ΔH is the enthalpy change per unit volume, $\dot{\epsilon}$ is the elongational strain rate, and

$$\dot{\epsilon} = (\nu_0/L)(\exp \epsilon_h - 1) \tag{29}$$

where ϵ_h is the Hencky strain, and $\epsilon_h = \ln (A_o/A_{ex})$. A_o is the initial area, A_{ex} is the exit area, L is the centerline length, and ν_o is the initial velocity.

The enthalpy change associated with what can at least be considered a flow-induced transformation to a metastable liquid crystalline form in various polymer systems can be estimated as follows. If the assumption is made that the non-Newtonian character of the fluid in excess of that reflected in η_s (at an equal shear rate) is due to the resistance to orientation, then the actual Trouton ratio would be $\eta_e/\eta_s = 3$. By measuring

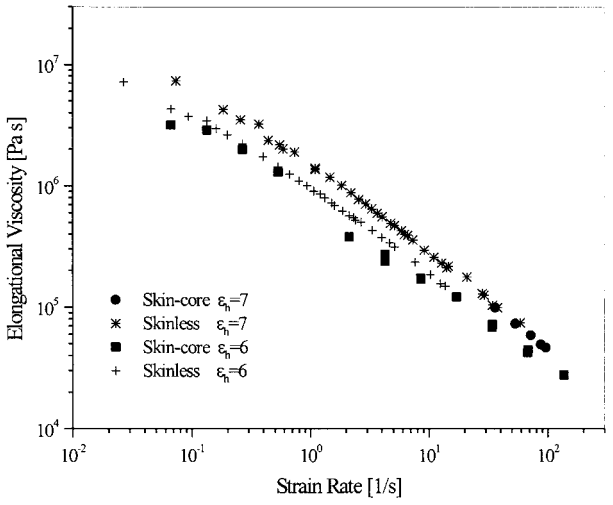

Figure 3 Lubricated and skinless polypropylene effective elongational viscosities.

η_s, then $\eta_e = 3\eta_s$, and substituting $3\eta_s$ into the above equations, enthalpy per unit volume, $\Delta H = \rho\Delta\hat{H}$, can be calculated from the resultant equation, as follows:

$$\Delta H = -\epsilon_h \dot{\epsilon}(\eta_{ef} - 3\eta_s) \tag{30}$$

The entropy change, ΔS, indicating the degree of orientation that develops, can be determined from $\Delta F = \Delta H - T\Delta S$, where ΔF is the Gibbs free energy, and T is the absolute temperature. If ΔF is assumed to be due to the flow-induced orientation, the transition to the metastable state is at equilibrium, then $\Delta F = 0$ and $\Delta S = (\Delta H/T)$.

RESULTS AND DISCUSSION

The effective elongational viscosity of skin–core PE–PP and skinless PP melts as a function of $\dot{\epsilon}$ are shown in Figure 3. Regression analysis results for both Hencky strains of 6 and 7 show that there are not statistically significant differences between the skin–core and skinless data. It should be noted that the PP skin–core data is more scattered than is the skinless data, probably because it is difficult to control the exact ratio of the skin to core layers.

Similar, but lower valued, elongational viscosity results occur for lyocell solutions. The dependence of the effective elongational viscosity of lyocell solutions upon temperature is shown in Figure 4 for a 17% solution of recycled cotton cellulose in the lyocell solvent, *N*-methylmorpholine oxide monohydrate (NMMO · H_2O) in the $\epsilon_h = 7$ die. The effective Trouton ratios η_{ef}/η_s (where η_s is the shear viscosity measured at the same temperature and at an equivalent magnitude shear rate) for this lyocell solution in this die vary from 3 (theoretical value for Newtonian behavior) at a $\dot{\epsilon}$ of 11.9 s^{-1} to 40 at a $\dot{\epsilon}$ of 94.0 s^{-1}. A liquid crystal phase

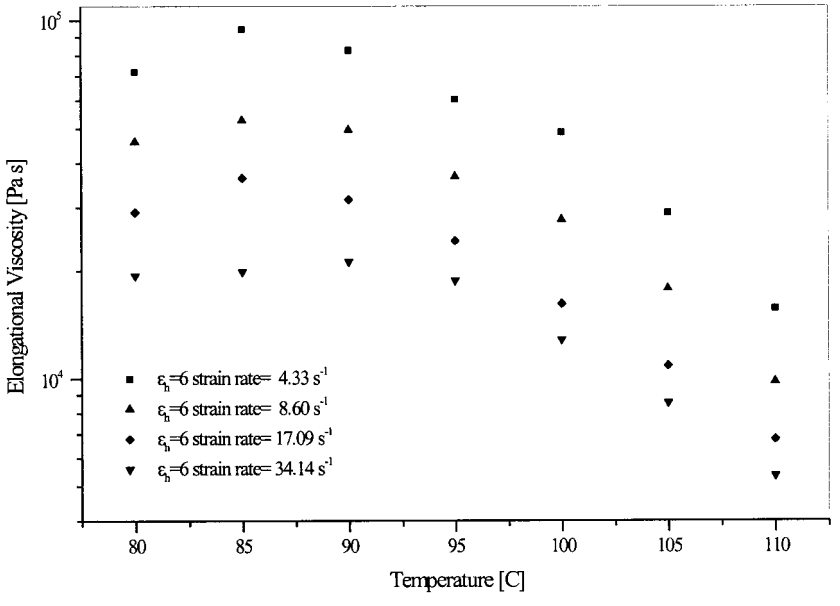

Figure 4 17% Recycled cotton lyocell effective elongational viscosities.

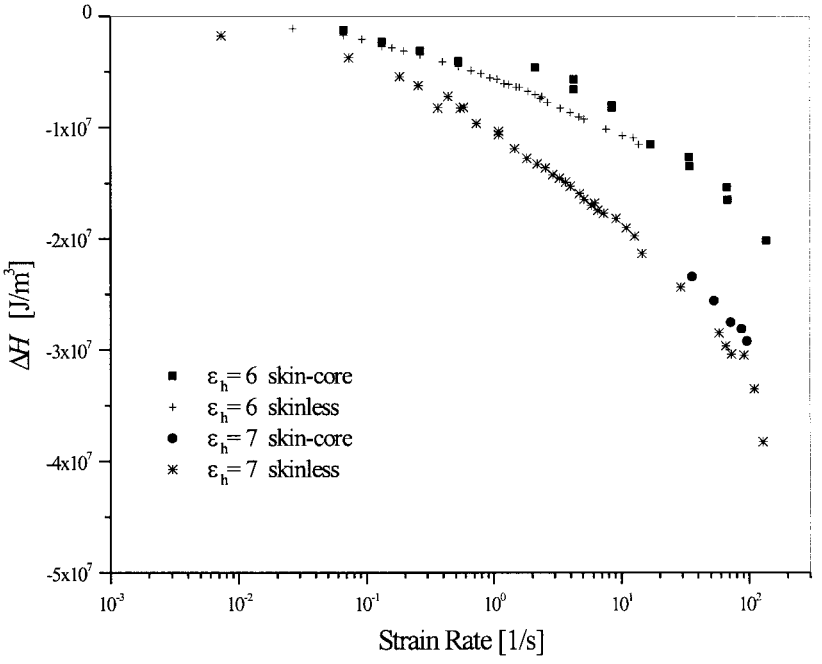

Figure 5 Polypropylene enthalpy change from rheology.

has been noted for this system, when quiescent,[14] in the range of 85 to 105°C and may be reflected in η_{ef}, with a local maximum around 85°C. The imposed pressures for elongational flow of this lyocell solution was, for $\epsilon_h = 7$, from 2.58 to 10.7 MPa for strain rates of 11.9 to 94.0 s^{-1} and temperatures from 80 to 110°C; the corresponding values for $\epsilon_h = 6$ were pressure from 0.75 to 4.33 MPa for strain rates of 4.3 to 34.1 s^{-1} and temperatures from 80 to 110°C.

Data from the flow behavior of PP and a 17% recycled cotton cellulose in an NMMO · H_2O solution illustrate the calculation of thermodynamic properties. The calculated enthalpy and entropy changes of polypropylene are shown in Figures 5 and 6, respectively. For PP at 200°C, the enthalpy change for the flow-induced transformation to a metastable state ranged from -1.03×10^7 to -3.83×10^7 J/m^3, with an increase in magnitude as $\dot{\epsilon}$ ranged from 1.1 to 128.0 s^{-1} and higher values for $\epsilon_h = 7$ than for $\epsilon_h = 6$. This can be compared to the enthalpy of fusion for polypropylene of -2.15×10^8 J/m^3, which is expected to be an order of magnitude higher since the solid crystalline state has a much higher degree of organization than does a low order liquid crystalline form.[17] The same trends were noted for the calculated entropy changes in PP, which ranged from -2.18×10^4 to -8.09×10^4 J K^{-1} m^{-3}. The data for a 17% recycled cotton cellulose in NMMO · H_2O at 95°C was comparable to the PP results with the same trends also exhibited. The enthalpy change for this cellulose solution, corrected for its concentration, ranged from -1.99×10^7 to -4.38×10^7 J/m^3, with an increase in magnitude as $\dot{\epsilon}$ ranged from 34.1 to 94.0 s^{-1} and higher values for $\epsilon_h = 7$ than for $\epsilon_h = 6$. The entropy ranged from -4.49×10^4 to -11.90×10^4 J K^{-1} m^{-3}. The preceding cellulose values are comparable to results for the same solution measured in a DSC: -0.44×10^6 to -4.38×10^7 J m^{-3} and -1.20×10^4 to -7.19×10^4 J K^{-1} m^{-3} for enthalpy and calculated entropy changes, respectively. It should be noted that the shear viscosity for this PP melt at the test temperature of 200°C is Newtonian until the shear rate is around 10^{-1} s^{-1}, and then it becomes shear-thinning, as shown in Figure 7. The ΔH and ΔS values are essentially zero below 10^{-1} s^{-1} and then they develop a dependence upon elongational strain rate.

As a result of the imposed pressures (1.15 to 42.60 MPa at elongational strain rates of 0.02 to 136.00 s^{-1}), the momentum balance equation suggested that significant body forces must be necessary to orient the fluid. Furthermore, the energy balance, expressed in terms of enthalpy for this controlled isothermal system, revealed a significant enthalpy change consistent with transformation to an ordered liquid crystalline

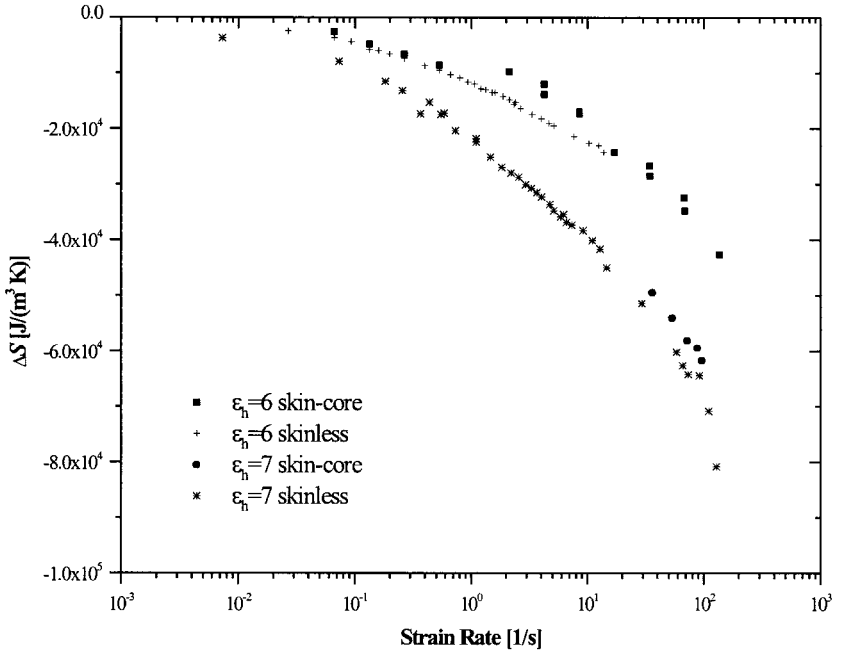

Figure 6 Polypropylene entropy change from rheology.

form (which may be metastable and induced due to flow). The suggestion of a transformation to an oriented liquid crystalline form by both calculated body forces and the enthalpy changes is consistent with earlier work on PP.[18] In the previous study, PP flowed through a linearly converging section of a die, then through a constant diameter section. A sharp temperature gradient was imposed on the latter section, thereby crystallizing the PP inside the die.[18] The die used in this earlier study was a standard Instron capillary die with a 90° linear tapered entrance with $\epsilon_h = 4$ for the machined entrance; if the flow-defined wine glass stem entrance pattern to the die from the specially designed reservoir were considered, then an effective ϵ_h would be approximately 7. These earlier PP samples exhibited 0.03-μm-diameter ultrafine filaments and an extremely high Herman–Stein orientation function (0.996, where 1.000 is perfect alignment in the flow direction, 0.000 is random, and −0.500 is transverse alignment).[18] Consistent with this earlier study and the calculated entropy change in this work, a high degree of alignment of cellulosic microfiber bundles resulted, as indicated in Figures 8 and 9, when they are formed from lyocell in elongational flow using the semihyperbolic convergent dies in this study. The sugar-cane-derived lyocell extrudate in Figure 8 indicates the orientation in the flow direction and organization into 10-μm structures, a similar one of which was separated and magnified in Figure 9 (from a 17% recycled cotton lyocell solution), and indicate 0.5-μm microfibers.[19]

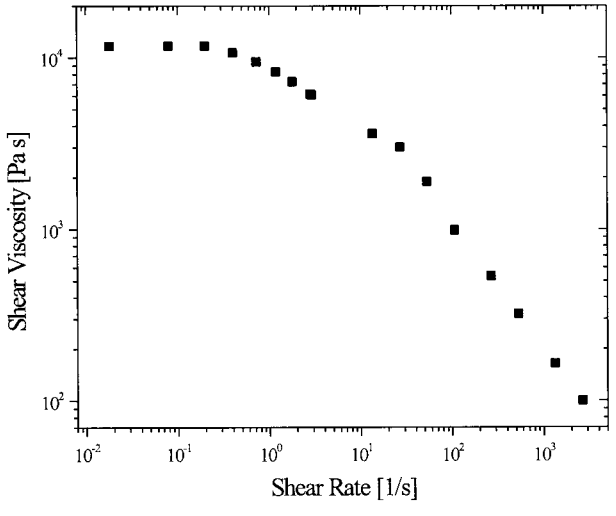

Figure 7 Polypropylene shear viscosities.

CONCLUSIONS

Elongational rheology of polymer melts and concentrated solutions using semihyperbolically con-

verging conical dies has demonstrated, at least for the PP melts and lyocell solutions tested, that the flow is dominated by the orientation developing in the fluid. Therefore, a skin layer of a lower viscosity fluid is neither necessary nor does the data require correction for shearing effects; the body forces related to the developing orientation are sufficiently strong to make the shearing gradient insignificant. The fluids are being transformed from an isotropic state to at least a metastable, oriented state. Retention of this orientation after exiting the dies would be dependent upon the relative rates of relaxation versus the induced phase change. The body forces related to this orientation development in cylindrical coordinates are

$$g_z = \frac{\partial P}{\partial z} \text{ and } g_r = \frac{\partial P}{\partial r}$$

and the associated enthalpy change is $\Delta H = -\epsilon_h \dot{\epsilon}(\eta_{ef} - 3\eta_s)$, where η_{ef}, the effective elongational viscosity is

$$\eta_{ef} = + \frac{\Delta P}{\dot{\epsilon}\epsilon_h}$$

Furthermore, by assuming that $\Delta F = 0$ for this transformation to an, at least, metastable state allows calculation of the entropy change, where $\Delta S = (\Delta H/T)$. The quantity $(\eta_{ef} - 3\eta_s)$ represents the excess non-Newtonian response of the fluids in elongational flow over what is represented by the shearing response at the same temperature and equivalent values of the shear rate. Therefore, the elongational rheology of polymer melts and concentrated solutions can be characterized in semihyperbolically ($R^2 z$ = constant) converging dies by measuring the volumetric flow rate and pressure drop through these dies. These results occur because the elongational strain rate $\dot{\epsilon}$ is constant in the dies, determined by the die geometry and volumetric flow rate.

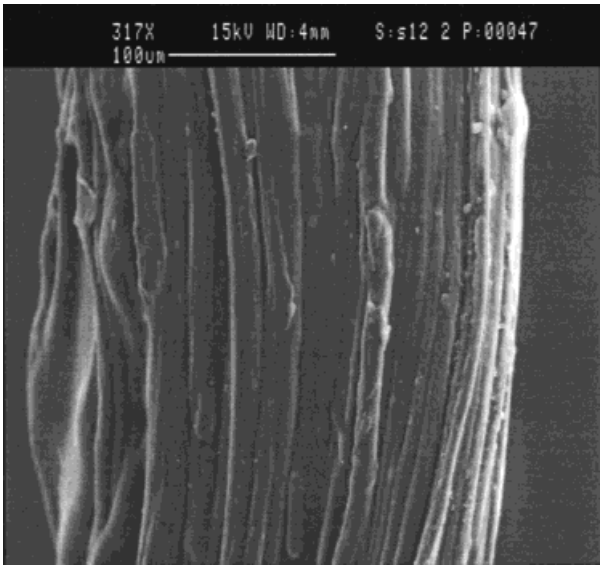

Figure 8 Sugar cane lyocell extrudate.

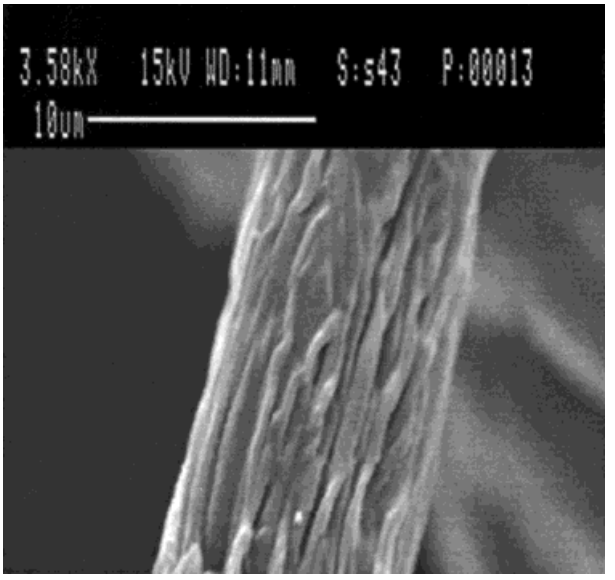

Figure 9 Recycled cotton lyocell microfiber tow.

REFERENCES

1. H. A. Barnes, J. F. Hutton, and K. Walters, *An Introduction to Rheology,* Elsevier, Amsterdam, 1989.
2. C. W. Macosko, *Rheology: Principles, Measurements, and Applications,* VCH, New York, 1994.
3. D. F. James, in *Recent Developments in Structured Continua,* D. DeKee and P. N. Kaloni, Eds., Longman, London, 1990.
4. J. Ferguson and Z. Kemblowski, *Applied Fluid Rheology,* New York, 1991.
5. J. R. Collier, U.S. Pat. 5,357,784 (1994).
6. A. V. Pendse and J. R. Collier, *J. Appl. Polym. Sci.,* **59,** 1305 (1996).
7. A. V. Pendse, PhD dissertation, Louisiana State University, 1995.
8. H. W. Kim, A. Pendse, and J. R. Collier, *J. Rheol.,* **38,** 831 (1994).
9. J. R. Collier, LSU Pat. Appl. OTT 9726 (1997).

10. H. Kwon, PhD dissertation, Louisiana State University, 1997.
11. O. Romanoschi, S. C. Romanoschi, J. R. Collier, and B. J. Collier, *Cell. Chem. Tech.,* **31,** 347 (1997).
12. H. Chanzy, M. Paillet, and A. Peguy, *Polym. Commun.,* **27,** 171 (1986).
13. H. Chanzy, B. Chumpatazi, and A. Peguy, *Carbohydr. Polym.,* **2,** 35 (1982).
14. P. Navard and J. M. Haudin, *Br. Polym. J.,* **12,** 174 (1980).
15. J. R. Collier and M. A. Perez, *Polym. Eng. Sci.,* **29,** 1004 (1989).
16. R. B. Bird, Warren E. Stewart, and Edwin N. Lightfoot, *Transport Phenomena,* Wiley, New York, 1960.
17. J. R. Collier, in *Problems in Materials Science,* M. D. Merchant, Ed., Gordon & Breach, New York, 1972.
18. J. R. Collier, T. Y. T. Tam, J. Newcome, and N. Dinos, *Polym. Eng. Sci.,* **16,** 204 (1976).
19. J. R. Collier, LSU Pat. Appl. OTT 9727 (1997).